Structural Engineering and Mechanics, *Vol. 65, No. 6 (2018) 721-730*
DOI: https://doi.org/10.12989/sem.2018.65.6.721

Adaptive control of rotationally non-linear asymmetric structures under seismic loads

Fereidoun Amini*[1], Hassan Rezazadeh[1a] and Majid Amin Afshar[2b]

[1]*School of Civil Engineering, Iran University of Science and Technology, P.O. Box 16765-163, Tehran, Iran*
[2]*Department of Technology and Engineering, Imam Khomeini International University Norouzian, P.O. Box 34149-16818, Qazvin, Iran*

(Received March 8, 2017, Revised January 3, 2018, Accepted January 19, 2018)

Abstract. This paper aims to inspect the effectiveness of the Simple Adaptive Control Method (SACM) to control the response of asymmetric buildings with rotationally non-linear behavior under seismic loads. SACM is a direct control method and was previously used to improve the performance of linear and non-linear structures. In most of these studies, the modeled structures were two-dimensional shear buildings. In reality, the building plans might be asymmetric, which cause the buildings to experience torsional motions under earthquake excitation. In this study, SACM is used to improve the performance of asymmetric buildings, and unlike conventional linear models, the non-linear inertial coupling terms are considered in the equations of motion. SACM performance is compared with the Linear Quadratic Regulator (LQR) algorithm. Moreover, the LQR algorithm is modified, so that it is appropriate for rotationally non-linear buildings. Active tuned mass dampers are used to improve the performance of the modeled buildings. The results show that SACM is successful in reducing the response of asymmetric buildings with rotationally non-linear behavior under earthquake excitation. Furthermore, the results of the SACM were very close to those of the LQR algorithm.

Keywords: rotational non-linearity; simple adaptive control method; active tuned mass damper; linear quadratic regulator; asymmetric buildings

1. Introduction

One of the most important goals of civil engineers is to reduce the response of the structures against dynamic loads like wind and earthquake (Bitaraf *et al.* 2010). Structural control in civil engineering has been proposed for more than four decades to improve the performance of the structures under earthquake excitation (Korkmaz 2011).

An adaptive control system is a control system with adjustable parameters, including a mechanism for adjusting these parameters (Housner *et al.* 1997). The Simple Adaptive Control Method (SACM) is a direct control method (Ozbulut *et al.* 2011) proposed by Sobel *et al.* (1982) and developed by Barkana and Kaufman (1993). In recent years, many researchers have implemented this method to control the response of structures under earthquake excitation. Bitaraf *et al.* (2010) studied the application of SACM to control the response of buildings with MR dampers subjected to earthquake. Ozbulut *et al.* (2011) used SACM to control the response of base isolated structures against near-field earthquakes. Amini and Javanbakht (2014) used SACM to control seismically excited structures with MR dampers. Bitaraf and Hurlebaus (2013) studied SACM to control a seismically excited 20-story non-linear building. It should be noted that the abovementioned researchers used two-dimensional building models.

SACM makes the controlled structure follow the behavior of a reference model. This method allows it to control structures with a lot of uncertainties (Bitaraf *et al.* 2010).

On the other hand, torsional motions have caused severe damages to asymmetric buildings in the past earthquakes (Amin Afshar and Amini 2012). Several researchers have studied the control of asymmetric buildings (Yoshida and Dyke 2005, Singh *et al.* 2002, Yoshida *et al.* 2003) but, they have used conventional linear equations of motion and they did not consider the non-linear inertial coupling terms in dynamic equations of motion. However, if these non-linear inertial coupling terms are considered, the building response may be quite different, and phenomena such as jumping, hysteresis and saturation may occur (Amin Afshar and Amini 2012). In this paper, the non-linear coupling terms in the dynamic equations of motion are considered and this type of non-linearity is called rotational (inertial) non-linearity.

The purpose of this study is to inspect the effectiveness of SACM to control the response of asymmetric buildings with rotational non-linearity under seismic excitation. SACM is used in a manner that is appropriate for rotationally non-linear buildings. Furthermore, the performance of SACM is compared with Linear Quadratic Regulator (LQR) algorithm. Here, two numerical examples, a five-story building and a fifteen-story building are

*Corresponding author, Professor
E-mail: famini@iust.ac.ir
[a]Research Assistant
E-mail: hrezazadeh1966@yahoo.com
[b]Ph.D.
E-mail: mafshar@eng.ikiu.ac.ir

ISSN: 1225-4568 (Print), 1598-6217 (Online)

presented. If rotational non-linearity is considered in the stated numerical examples, the response of the modeled buildings will be different from the conventional linear approach. Active Tuned Mass Damper (ATMD) is used to improve the performance of these buildings under earthquake excitation.

2. Non-linear differential equations of motion

As shown in Fig. 1, a single-story building with a rigid diaphragm is subjected to earthquake excitation in X and Y directions. The floor center of mass is represented by C.M., and C.R. denotes the center of stiffness of the story. As seen in Fig. 2, two coordinates systems are defined. The first coordinates system is the global XYZ, which is fixed on the ground, and the second coordinates system is the local rotary xyz, which is attached to the floor center of mass. Based on the Amini and Amin Afshar (2011) approach, the non-linear equations of motion in the local xyz coordinates system are as follows

$$m\ddot{u}_x + C_x\dot{u}_x + K_x u_x = -m(-2\dot{u}_y\dot{\theta} - u_y\ddot{\theta} - u_x\dot{\theta}^2 + \ddot{u}_{gX}\cos\theta + \ddot{u}_{gY}\sin\theta) \quad (1)$$

$$m\ddot{u}_y + C_y\dot{u}_y + K_y u_y + e_x K_y\theta = -m(2\dot{u}_x\dot{\theta} + u_x\ddot{\theta} - u_y\dot{\theta}^2 - \ddot{u}_{gX}\sin\theta + \ddot{u}_{gY}\cos\theta) \quad (2)$$

$$mr^2\ddot{\theta} + C_\theta\dot{\theta} + (K_{\theta R} + K_y e_x^2)\theta + e_x K_y u_y = 0 \quad (3)$$

In the above equations, e_x is the eccentricity between the story center of mass and center of stiffness in x direction. Also, it is assumed that C.R. lies on the X axis. The parameter e_x can be calculated by

$$e_x = \frac{\sum_{j=1}^{N} x_j k_{yj}}{\sum_{j=1}^{N} k_{yj}} \quad (4)$$

where k_{yj} denotes the stiffness of the jth element resisting in Y direction and the parameter N represents the number of resisting elements in Y direction.

In Eqs. (1)-(3), the parameter m is the total mass of the floor and r is the floor radius of gyration about the center of mass, $\ddot{u}_{gX}$ and $\ddot{u}_{gY}$ are the earthquake accelerations in X and Y directions, u_x and u_y are displacements of the floor center of mass in the x and y directions, and θ is the torsional rotation of the floor about the z axis. Also, K_x and K_y are the sum of the story resisting elements stiffness in x and y directions. The parameter $K_{\theta R}$ is the torsional stiffness of the story about C.R., and can be calculated by

$$K_{\theta R} = \sum_{j=1}^{M} K_{xj} y_j^2 + \sum_{j=1}^{N} K_{yj}(x_j - e_x)^2 \quad (5)$$

where K_{xj} is the stiffness of the jth resisting element in X direction and the parameter M represents the number of resisting elements in X direction. Also, C_x, C_y and C_θ are damping coefficients.

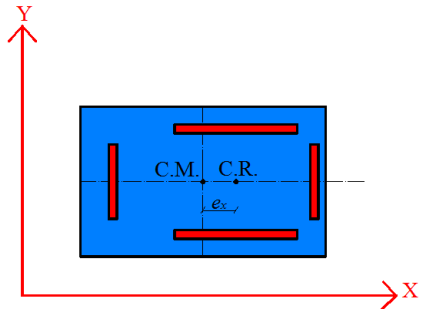

Fig. 1 Asymmetric plan of a single-story building; structure elements (beams and columns)

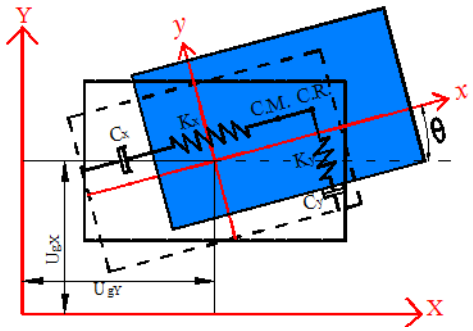

Fig. 2 Global (XYZ) and local (xyz) coordinates systems

Now for a multi-story building, the equations of motion for the ith floor can be expressed as

$$M_i a_i^i + C_i^i\dot{\bar{U}}_i^i + K_i^i\bar{U}_i^i - C_{i+1}^i\dot{\bar{U}}_{i+1}^i - K_{i+1}^i\bar{U}_{i+1}^i = 0 \quad (6)$$

The above equation is derived in the rotary $x_iy_iz_i$ system of coordinates. As shown in Fig. 3, the $x_iy_iz_i$ system of coordinates is located on the base of the building and it rotates about the z_i axis by an angle θ_i. The variable θ_i is the total rotation of the ith floor about the z_i axis. Also, as seen in Fig. 3, the XYZ system of coordinates is fixed on the ground. In Eq. (6), M_i represents the mass matrix of the ith floor, and can be expressed as the following 3×3 matrix

$$M_i = \begin{bmatrix} m_i & 0 & 0 \\ 0 & m_i r_i^2 & 0 \\ 0 & 0 & m_i \end{bmatrix} \quad (7)$$

In the above formula, m_i is the total mass of the ith floor and r_i is the ith floor radius of gyration about the center of mass. Also, in Eq. (6), a_i^i denotes the total acceleration of the ith floor center of mass in the local $x_iy_iz_i$ coordinates system, which is given by (Beer *et al.* 2013)

$$a_i^i = \begin{Bmatrix} a_{xi}^i \\ a_{\theta i} \\ a_{yi}^i \end{Bmatrix} = \begin{Bmatrix} \ddot{u}_{xi}^i \\ \ddot{\theta}_i \\ \ddot{u}_{yi}^i \end{Bmatrix} + \begin{Bmatrix} -2\dot{u}_{yi}^i\dot{\theta}_i - u_{yi}^i\ddot{\theta}_i - u_{xi}^i\dot{\theta}_i^2 \\ 0 \\ 2\dot{u}_{xi}^i\dot{\theta}_i + u_{xi}^i\ddot{\theta}_i - u_{yi}^i\dot{\theta}_i^2 \end{Bmatrix} + \begin{Bmatrix} \ddot{U}_{Xg}\cos\theta_i + \ddot{U}_{Yg}\sin\theta_i \\ 0 \\ -\ddot{U}_{Xg}\sin\theta_i + \ddot{U}_{Yg}\cos\theta_i \end{Bmatrix} \quad (8)$$

In above equation, u_{xi}^{i} and u_{yi}^{i} are displacements of the *i*th floor center of mass in x_i and y_i directions and θ_i is the torsional rotation of the *i*th floor about the z_i axis (see Fig. 3); $\ddot{U}_{Xg}$ and $\ddot{U}_{Yg}$ are the ground translational accelerations in *X* and *Y* directions; $-2\dot{u}_{yi}^{i}\dot{\theta}_i$ and $2\dot{u}_{xi}^{i}\dot{\theta}_i$ are known as Coriolis components of the acceleration; $-u_{yi}^{i}\ddot{\theta}_i$ and $u_{xi}^{i}\ddot{\theta}_i$ denote the tangential components of the acceleration; $-u_{xi}^{i}\dot{\theta}_i^2$ and $-u_{yi}^{i}\dot{\theta}_i^2$ are the centrifugal components of the acceleration. In Eq. (6), K_i^i is the stiffness matrix of the *i*th story and is defined in the directions of the $x_iy_iz_i$ coordinates system. The matrix K_i^i can be expressed as

$$K_i^i = \begin{bmatrix} K_{xi}^i & 0 & 0 \\ 0 & K_{\theta i} & K_{yi}^i e_{xi} \\ 0 & K_{yi}^i e_{xi} & K_{yi}^i \end{bmatrix} \tag{9}$$

where K_{xi}^{i} and K_{yi}^{i} are the *i*th story total stiffness in the x_i and y_i directions. As seen in Fig. 4, the parameters K_{xi}^{i} and K_{yi}^{i} are defined in the local $x_iy_iz_i$ coordinates system. The parameter $K_{\theta i}^{i}$ is the torsional stiffness of the *i*th story about the *i*th story center of stiffness. Also, e_{xi} is the eccentricity between the center of mass and center of stiffness of the *i*th story in x_i direction.

Furthermore in Eq. (6), C_i^i is the damping matrix of the *i*th story and is defined in the directions of the $x_iy_iz_i$ coordinates system. Matrix C_i^i can be expressed as

$$C_i^i = \begin{bmatrix} C_{xi}^i & 0 & 0 \\ 0 & C_{\theta i} & C_{yi}^i e_{xi} \\ 0 & C_{yi}^i e_{xi} & C_{yi}^i \end{bmatrix} \tag{10}$$

where C_{xi}^{i}, C_{yi}^{i} and $C_{\theta i}$ are the *i*th story damping coefficients, which are defined in the directions of the local $x_iy_iz_i$ coordinates system (see Fig. 4).

If U_{Xi} and U_{Yi} denote the displacements of the *i*th floor center of mass in *X* and *Y* directions (see Fig. 3), and θ_i denotes the *i*th floor rotation about the z_i axis, the relationship between $\left[U_{Xi}, \theta_i, U_{Yi}\right]^T$ and $\left[u_{xi}, \theta_i, u_{yi}\right]^T$ vectors can be expressed as

$$U_i^i = \begin{Bmatrix} u_{xi}^i \\ \theta_i \\ u_{yi}^i \end{Bmatrix} = \begin{bmatrix} \cos\theta_i & 0 & \sin\theta_i \\ 0 & 1 & 0 \\ -\sin\theta_i & 0 & \cos\theta_i \end{bmatrix} \begin{Bmatrix} U_{Xi} \\ \theta_i \\ U_{Yi} \end{Bmatrix} = Q^i U^i \tag{11}$$

where Q^i is the rotation matrix about the z_i axis by an angle θ_i.

Moreover, the vector U_{i+1}^{i+1} is defined by

$$U_{i+1}^{i+1} = \left[u_{x_{i+1}}^{i+1}, \theta_{i+1}, u_{y_{i+1}}^{i+1}\right]^T \tag{12}$$

Also in Eq. (6), $\bar{U}_i^i$ and $\bar{U}_{i+1}^{i}$ are defined by

$$\bar{U}_i^i = U_i^i - U_{i-1}^i \tag{13}$$

$$\bar{U}_{i+1}^i = U_{i+1}^i - U_i^i \tag{14}$$

In the above equations, U_{i-1}^{i} denotes the *i-1*th floor displacement vectors. Furthermore, U_{i+1}^{i} is the *i+1*th floor displacement vector. The vectors U_{i-1}^{i} and U_{i+1}^{i}, are defined in the $x_iy_iz_i$ coordinates system. The relationship between U_{i+1}^{i} and U_{i+1}^{i+1} can be expressed in the following equation

$$U_{i+1}^i = \begin{Bmatrix} u_{xi+1}^i \\ \theta_{i+1} \\ u_{yi+1}^i \end{Bmatrix} = \begin{bmatrix} \cos\bar{\theta}_{i+1} & 0 & -\sin\bar{\theta}_{i+1} \\ 0 & 1 & 0 \\ \sin\bar{\theta}_{i+1} & 0 & \cos\bar{\theta}_{i+1} \end{bmatrix} \begin{Bmatrix} u_{xi+1}^{i+1} \\ \theta_{i+1} \\ u_{yi+1}^{i+1} \end{Bmatrix} = (\bar{Q}_i^{i+1})^T u_{i+1}^{i+1} \tag{15}$$

where $\bar{\theta}_{i+1}$ is defined as follows

$$\bar{\theta}_{i+1} = \theta_{i+1} - \theta_i \tag{16}$$

Also, in Eq. (15), $\bar{Q}_i^{i+1}$ is the rotation matrix about the z_i axis by an angle $\bar{\theta}_{i+1}$.

Matrix K_{i+1}^{i} can now be derived from Eq. (6). The vector F_{i+1}^{i+1} is defined by

$$F_{i+1}^{i+1} = K_{i+1}^{i+1}\bar{U}_{i+1}^{i} \tag{17}$$

Vector F_{i+1}^{i+1}, denotes the force of the resisting elements in *i+1*th story, which is exerted to the *i+1*th floor. It should be noted that vector F_{i+1}^{i+1} is defined in the $x_{i+1}y_{i+1}z_{i+1}$ system of coordinates. Evidently the reaction of F_{i+1}^{i+1} is exerted to the *i*th floor. To define the vector F_{i+1}^{i+1} reaction in the $x_iy_iz_i$ coordinates system, the $x_{i+1}y_{i+1}z_{i+1}$ coordinates system can be rotated about the z_i axis by an angle $-\bar{\theta}_{i+1}$. The following equation can thus be written

$$F_{i+1}^{i} = -\left(\bar{Q}_i^{i+1}\right)^T F_{i+1}^{i+1} \tag{18}$$

where vector F_{i+1}^{i} is the reaction of the vector F_{i+1}^{i+1} which is defined in the $x_iy_iz_i$ coordinates system. On the other hand, in Eq. (6) vector F_{i+1}^{i} is defined by

$$F_{i+1}^{i} = -K_{i+1}^{i}\bar{U}_{i+1}^{i} \tag{19}$$

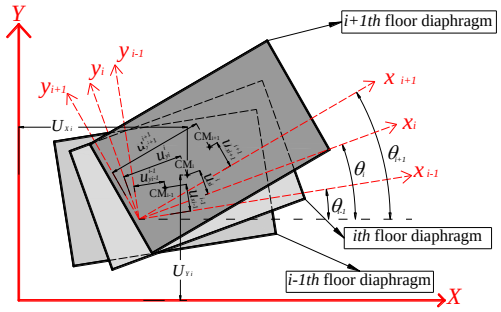

Fig. 3 Rotary $x_iy_iz_i$ coordinates system is located on the base of the building, and rotates about the z_i axis by an angle θ_i; CM_i denotes the ith floor center of mass

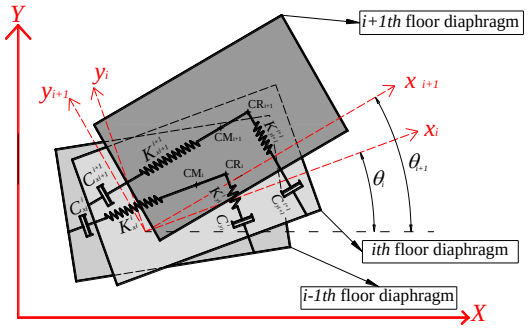

Fig. 4 The stiffness and damping of the ith story are defined in local $x_iy_iz_i$ system of coordinates; CR_i denotes the ith story center of stiffness

According to Eqs. (17)-(19), the term $-K_{i+1}^{i}\bar{U}_{i+1}^{i}$ can be expressed as

$$\begin{aligned}-K_{i+1}^{i}\bar{U}_{i+1}^{i} &= F_{i+1}^{i} = -\left(\bar{Q}_i^{i+1}\right)^T F_{i+1}^{i+1} = \\ -\left(\bar{Q}_i^{i+1}\right)^T K_{i+1}^{i+1}\left(\bar{U}_{i+1}^{i+1}\right) &= -\left(\bar{Q}_i^{i+1}\right)^T K_{i+1}^{i+1}\left(\bar{Q}_i^{i+1}\left(\bar{U}_{i+1}^{i}\right)\right) \\ &= -\left(\left(\bar{Q}_i^{i+1}\right)^T K_{i+1}^{i+1}\left(\bar{Q}_i^{i+1}\right)\right)\bar{U}_{i+1}^{i}\end{aligned} \quad (20)$$

K_{i+1}^{i} can therefore, be obtained by the following equation

$$K_{i+1}^{i} = \left(\bar{Q}_i^{i+1}\right)^T K_{i+1}^{i+1}\left(\bar{Q}_i^{i+1}\right) \quad (21)$$

The same procedure can be used to derive C_{i+1}^{i}, and it can be calculated by

$$C_{i+1}^{i} = \left(\bar{Q}_i^{i+1}\right)^T C_{i+1}^{i+1}\left(\bar{Q}_i^{i+1}\right) \quad (22)$$

where C_{i+1}^{i+1} is the $i+1$th floor damping matrix defined in $x_{i+1}y_{i+1}z_{i+1}$ coordinates system.

3. Simple adaptive control method

The controlled structure (plant) output in SACM is compared with the reference model output (Bitaraf and Hurlebaus 2013), and the objective of this method is to reduce the difference between output of the controlled structure (plant) and reference model (Ozbulut *et al.* 2011). Furthermore, the order of the reference model state in SACM can be less than the order of the plant state. The state space equations of a non-linear plant can be represented by (Bitaraf and Hurlebaus 2013)

$$\dot{x}_p(t) = A_p(x_p)x_p(t) + B_p(x_p)u_p(t) + d_i(x_p,t) \quad (23)$$

$$y_p(t) = C_p(x_p)x_p(t) + D_p(x_p)u_p(t) + d_0(x_p,t) \quad (24)$$

Here, the non-linear behavior of the structure is caused by taking the non-linear inertial coupling terms in the dynamic equations of motion into consideration. Also, the behavior of the reference model can be represented by (Bitaraf and Hurlebaus 2013)

$$\dot{x}_m(t) = A_m(x_m)x_m(t) + B_m(x_m)u_m(t) \quad (25)$$

$$y_m(t) = C_m(x_m)x_m(t) + D_m(x_m)u_m(t) \quad (26)$$

In above equations A_p and A_m are state matrices, B_p and B_m are input matrices, and C_p and C_m are output matrices for the plant and reference model (Bitaraf *et al.* 2012). Moreover, x_p is the $2n\times1$ plant state vector and x_m is the $2n_m\times1$ reference model state vector. Also, y_m and y_p represent the reference model output and the plant output (Bitaraf and Hurlebaus 2013).

The control command is denoted by u_p and the input command is denoted by u_m. The control command and input command are $m\times1$ vectors (Bitaraf *et al.* 2010). It should be noted that y_p and y_m are m-order vectors and must have an equal order. Also, d_i and d_0 denote input and output disturbances (Bitaraf and Hurlebaus 2013). If the parameter $D_p(x_p)$ is very small, it may not affect the plant output but it can considerably change the stability characteristics of the plant (Bitaraf and Hurlebaus 2013, Barkana and Guez 1990).

The control command $m\times1$ vector can be calculated by (Bitaraf *et al.* 2010, Bitaraf and Hurlebaus 2013)

$$u_p = K(t)\left[y_m - y_p \quad x_m^T(t) \quad u_m^T(t)\right]^T = K(t)r(t) \quad (27)$$

The overall gain $K(t)$ is

$$\begin{aligned}K(t) &= \left[K_e(t) \quad K_x(t) \quad K_u(t)\right] \\ &= K_I(t) + K_P(t)\end{aligned} \quad (28)$$

As written in Eq. (28), the overall gain is the sum of the integral gain $K_I(t)$ and the proportional gain $K_P(t)$. The matrices $K_I(t)$ and $K_P(t)$ can be calculated by (Bitaraf *et al.* 2010)

$$\dot{K}_I(t) = \left(y_m(t) - y_p(t)\right)r^T(t)T - \sigma_{SAC}K_I(t) \quad (29)$$

$$K_P(t) = \left(y_m(t) - y_p(t)\right)r^T(t)\bar{T} \quad (30)$$

The use of the coefficient σ_{SAC} in Eq. (29) prevents the

integral gain from attaining very high values (Ozbulut *et al.* 2011). The positive definite matrices $\overline{T}$ and T control the rate of adaptation. The proportional gain is used to improve the convergence rate of the plant output to the reference model output. The integral gain is essential to make the system stable (Bitaraf *et al.* 2010).

In this research and in SACM, it is assumed that the input earthquake excitation is unknown. If the input command u_m is zero, there is no need to know the input excitation. In this case, the model state vector can be calculated as follows (Bitaraf and Hurlebaus 2013)

$$x_m = \begin{bmatrix} X_m \\ \dot{X}_m \end{bmatrix} = \begin{bmatrix} \int \dot{X}_m dt \\ \dot{X}_m \end{bmatrix} = \begin{bmatrix} \int y_m dt \\ y_m \end{bmatrix} \tag{31}$$

where X_m and $\dot{X}_m$ are displacement and velocity of the reference model.

In this study, the reference model is a structure having the output in a specified range. The behavior of the reference model is explained by (Bitaraf *et al.* 2010, Bitaraf and Hurlebaus 2013)

$$\begin{aligned} y_m &= y_p \quad \text{if} \quad |y_p| < Y_{\max} \\ y_m &= Y_{\max} \quad \text{if} \quad |y_p| \geq Y_{\max} \end{aligned} \tag{32}$$

where Y_{max} denotes the maximum acceptable value for the output of the reference model. The value of Y_{max} can be equal to or greater than zero (Bitaraf *et al.* 2010). If the output of the plant is less than Y_{max}, the difference between the plant and reference model output is zero, and if the plant output is more than Y_{max}, the objective of SACM is to reduce the difference between the plant and reference model output (Bitaraf and Hurlebaus 2013). In this paper, the output of the plant is the velocity of each controlled degree of freedom (Bitaraf *et al.* 2010, Bitaraf and Hurlebaus 2013).

4. Linear quadratic regulator algorithm

The performance of the SACM will be compared with the well-known LQR algorithm. To use the LQR algorithm, the equations of motion are derived in state space form. The plant state space equations are given by Eqs. (23)-(24). In Eq. (23), the parameter $x_p(t)$ is defined by

$$\begin{aligned} x_p(t) = \Big[&\left(U^1\right)^T, \left(U^2\right)^T, ..., \left(U^{n_f}\right)^T, \\ &\left(\dot{U}^1\right)^T, \left(\dot{U}^2\right)^T, ..., \left(\dot{U}^{n_f}\right)^T \Big]^T \end{aligned} \tag{33}$$

As mentioned in Section 2, U^i is the displacement vector of the ith floor which is defined in the global XYZ coordinates system (see Fig. 3). Also, n_f is the number of the modeled building stories.

Now, in Eq. (23), the matrices A_p, B_p and d_i will be derived. These matrices will be derived according to Eq. (6). Based on Eqs. (11), (13) and (15), in Eq. (6), the term $K_i^i \overline{U}_i^i$ can be expressed as

$$\begin{aligned} K_i^i \overline{U}_i^i &= K_i^i \left(U_i^i - U_{i-1}^i\right) = K_i^i \left(U_i^i - \overline{Q}_{i-1}^i U_{i-1}^{i-1}\right) \\ &= K_i^i \left(\left(Q^i\right)^T U^i - \overline{Q}_{i-1}^i \left(Q^{i-1}\right)^T U^{i-1}\right) \end{aligned} \tag{34}$$

The matrix K^+ is defined as follows

$$K^+ = \begin{bmatrix} K_1^1 & 0 & 0 & 0 \\ 0 & K_2^2 & 0 & 0 \\ 0 & 0 & ... & 0 \\ 0 & 0 & 0 & K_{n_f}^{n_f} \end{bmatrix} \tag{35}$$

Also, the matrices q, q^- and q^+ are defined by

$$q = \begin{bmatrix} \left(Q^1\right)^T & 0 & 0 & 0 \\ 0 & \left(Q^2\right)^T & 0 & 0 \\ 0 & 0 & ... & 0 \\ 0 & 0 & 0 & \left(Q^{n_f}\right)^T \end{bmatrix} \tag{36}$$

$$q^- = \begin{bmatrix} 0 & 0 & 0 & 0 & 0 \\ \overline{Q}_1^2 & 0 & 0 & 0 & 0 \\ 0 & \overline{Q}_2^3 & 0 & 0 & 0 \\ 0 & 0 & \cdots & 0 & 0 \\ 0 & 0 & 0 & \overline{Q}_{n_f-1}^{n_f} & 0 \end{bmatrix} \tag{37}$$

$$q^+ = \begin{bmatrix} 0 & \left(\overline{Q}_1^2\right)^T & 0 & 0 & 0 \\ 0 & 0 & \left(\overline{Q}_2^3\right)^T & 0 & 0 \\ 0 & 0 & 0 & ... & 0 \\ 0 & 0 & 0 & 0 & \left(\overline{Q}_{n_f-1}^{n_f}\right)^T \\ 0 & 0 & 0 & 0 & 0 \end{bmatrix} \tag{38}$$

As mentioned in Section 2, K_i^i, Q^i, Q_i^{i+1} are 3×3 matrices. It is obvious that K^+, q, q^- and q^+ are $3n_f\times3n_f$ matrices. The following equation can be derived from Eq. (34)

$$\begin{aligned} &\left[\left(K_1^1 \overline{U}_1^1\right)^T, \left(K_2^2 \overline{U}_2^2\right)^T, ..., \left(K_{n_f}^{n_f} \overline{U}_{n_f}^{n_f}\right)^T\right]^T = \\ &K^+ \times \left(q - q^- \times q\right) \times \left[\left(U^1\right)^T, \left(U^2\right)^T, \cdots, \left(U^{n_f}\right)^T\right]^T \end{aligned} \tag{39}$$

Based on Eqs. (11), (15) and (21), the term $K_{i+1}^i \overline{U}_{i+1}^i$ in Eq. (6) can be expressed as

$$\begin{aligned} &K_{i+1}^i \overline{U}_{i+1}^i = \\ &\left(\overline{Q}_i^{i+1}\right)^T K_{i+1}^{i+1} \left(\overline{Q}_i^{i+1}\right) \left((\overline{Q}_i^{i+1})^T U_{i+1}^{i+1} - U_i^i\right) = \\ &\left(\overline{Q}_i^{i+1}\right)^T K_{i+1}^{i+1} \left(\overline{Q}_i^{i+1}\right) \left((\overline{Q}_i^{i+1})^T \left(Q^{i+1}\right)^T U^{i+1} - \left(Q^i\right)^T U^i\right) \end{aligned} \tag{40}$$

The following equation can be derived from the above equation

$$\left[\left(K_2^1\bar{U}_2^1\right)^T,\left(K_3^2\bar{U}_3^2\right)^T,....,\left(K_{n_f}^{n_f-1}\bar{U}_{n_f}^{n_f-1}\right)^T\right]^T = \left(q^+\right)\times K^+\times\left(q^-\right)\times\left(q^+\times q-q\right) \times\left[\left(U^1\right)^T,\left(U^2\right)^T,\cdots,\left(U^{n_f}\right)^T\right]^T \tag{41}$$

Similar to Eqs. (39) and (41), the following equations can be derived

$$\left[\left(C_1^1\dot{\bar{U}}_1^1\right)^T,\left(K_2^2\dot{\bar{U}}_2^2\right)^T,....,\left(K_{n_f}^{n_f}\dot{\bar{U}}_{n_f}^{n_f}\right)^T\right]^T = C^+\times\left(q-q^-\times q\right)\times\left[\left(\dot{U}^1\right)^T,\left(\dot{U}^2\right)^T,\cdots,\left(\dot{U}^{n_f}\right)^T\right]^T \tag{42}$$

$$\left[\left(C_2^1\dot{\bar{U}}_2^1\right)^T,\left(C_3^2\dot{\bar{U}}_3^2\right)^T,....,\left(C_{n_f}^{n_f-1}\dot{\bar{U}}_{n_f}^{n_f-1}\right)^T\right]^T = \left(q^+\right)\times C^+\times\left(q^-\right)\times\left(q^+\times q-q\right) \times\left[\left(\dot{U}^1\right)^T,\left(\dot{U}^2\right)^T,\cdots,\left(\dot{U}^{n_f}\right)^T\right]^T \tag{43}$$

where C^+ is defined by

$$C^+=\begin{bmatrix} C_1^1 & 0 & 0 & 0\\ 0 & C_2^2 & 0 & 0\\ 0 & 0 & ... & 0\\ 0 & 0 & 0 & C_{n_f}^{n_f}\end{bmatrix} \tag{44}$$

Moreover, vector a_i^i in Eq. (6) can be expressed as

$$a_i^i=\left(Q^i\right)^T\ddot{U}^i \tag{45}$$

and following equation can be derived

$$\left[\left(M_1a_1^1\right)^T,\left(M_2a_2^2\right)^T,....,\left(M_{n_f}a_{n_f}^{n_f}\right)^T\right]^T = M^+\times q\times\left[\left(\ddot{U}^1\right)^T,\left(\ddot{U}^2\right)^T,....,\left(\ddot{U}^{n_f}\right)^T\right]^T \tag{46}$$

where M^+ is defined by

$$M^+=\begin{bmatrix} M_1 & 0 & 0 & 0\\ 0 & M_2 & 0 & 0\\ 0 & 0 & ... & 0\\ 0 & 0 & 0 & M_{n_f}\end{bmatrix} \tag{47}$$

Now, in Eq. (23), matrix $A_p(x_p)$ can is expressed as

$$A_p(x_p)=\begin{bmatrix} 0_{3n_f\times 3n_f} & I_{3n_f\times 3n_f}\\ A_{p_{21}} & A_{p_{22}}\end{bmatrix} \tag{48}$$

According to Eqs. (6), (39), (41)-(43) and (45), $A_{p_{21}}$ and $A_{p_{22}}$ are expressed as

$$A_{p_{21}}=q^{-1}\times\left(M^+\right)^{-1}\times\left[K^+\times\left(q-q^-\times q\right) -\left(q^+\right)\times K^+\times\left(q^-\right)\times\left(q^+\times q-q\right)\right] \tag{49}$$

$$A_{p_{22}}=q^{-1}\times\left(M^+\right)^{-1}\times\left[C^+\times\left(q-q^-\times q\right) -\left(q^+\right)\times C^+\times\left(q^-\right)\times\left(q^+\times q-q\right)\right] \tag{50}$$

It is obvious that matrix A_p is not constant through the excitation, and matrix $I_{3n_f\times 3n_f}$, is the identity matrix.

Moreover, in Eq. (23), the matrices $B_p(x_p)$ and $d_i(x_p, t)$ are given by

$$B_p(x_p)=\begin{bmatrix} 0\\ \left(M^+\right)^{-1}D\end{bmatrix} \tag{51}$$

$$d_i(x_p,t)=\begin{bmatrix} 0\\ \left(M^+\right)^{-1}\end{bmatrix}\times f(t) \tag{52}$$

In the above equations, D is the control device location matrix, and f is the external loading vector which is given by following $3n_f\times 1$ matrix

$$f(\mathrm{t})=\left[-m_1\ddot{U}_{Xg},0,-m_1\ddot{U}_{Yg},-m_2\ddot{U}_{Xg},0 ,-m_2\ddot{U}_{Yg},...,-m_{n_f}\ddot{U}_{Xg},0,-m_{n_f}\ddot{U}_{Yg}\right]^T \tag{53}$$

The objective function in the LQR algorithm is defined by (Khansefid and Ahmadizadeh 2015)

$$J=\int_0^t\left[\left(x_p(t)\right)^TQx_p(t)+\left(u_p(t)\right)^TRu_p(t)\right]dt \tag{54}$$

where Q is the positive semi-definite weighting matrix of displacement and R is the positive definite matrix of the control force. The control forces in the LQR algorithm are calculated in a manner that minimizes the objective function. In this algorithm, the control command vector, $u_p(t)$ is calculated by (Nazarimofrad and Zahrai 2016)

$$u_p(t)=Gx_p(t)=\left(-\frac{1}{2}R^{-1}B^TP\right)x_p(t) \tag{55}$$

In above equation, G is the control gain matrix and matrix P is determined by solving following non-linear Riccati equation (Khansefid and Ahmadizadeh 2016)

$$PA_p-\frac{1}{2}PBR^{-1}B^TP+A_p{}^TP+2Q=0 \tag{56}$$

In this study, it is assumed that the control gain matrix is not constant through the excitation. The Riccati equation is solved and the control gain matrix is updated in every time step. Also, in Eq. (54), the matrices Q and R are assumed to

Table 1 Modeled buildings properties

Story number	five-story building						fifteen-story					
	Mass	K_x	K_y	$K_{\theta R}$	e_x	r	Mass	K_x	K_y	$K_{\theta R}$	e_x	r
	($N.s^2/cm$)	(N/cm)	(N/cm)	($N.cm$)	(cm)	(cm)	($N.s^2/cm$)	(N/cm)	(N/cm)	($N.cm$)	(cm)	(cm)
1	0.1	142.1	142.1	32095	9.67	20	0.25	3869	3869	2751800	17.5	35
2	0.1	142.1	142.1	32095	9.67	20	0.25	3869	3869	2751800	17.5	35
3	0.1	142.1	142.1	32095	9.67	20	0.25	3869	3869	2751800	17.5	35
4	0.1	142.1	142.1	32095	9.67	20	0.25	3869	3869	2751800	17.5	35
5	0.1	142.1	142.1	32095	9.67	20	0.25	3869	3869	2751800	17.5	35
6	-	-	-	-	-	-	0.25	3095	3095	2201400	17.5	35
7	-	-	-	-	-	-	0.25	3095	3095	2201400	17.5	35
8	-	-	-	-	-	-	0.25	3095	3095	2201400	17.5	35
9	-	-	-	-	-	-	0.25	3095	3095	2201400	17.5	35
10	-	-	-	-	-	-	0.25	3095	3095	2201400	17.5	35
11	-	-	-	-	-	-	0.25	2321	2321	1651100	17.5	35
12	-	-	-	-	-	-	0.25	2321	2321	1651100	17.5	35
13	-	-	-	-	-	-	0.25	2321	2321	1651100	17.5	35
14	-	-	-	-	-	-	0.25	2321	2321	1651100	17.5	35
15	-	-	-	-	-	-	0.25	2321	2321	1651100	17.5	35

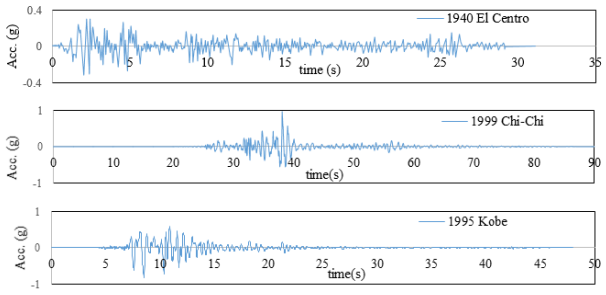

Fig. 5 Earthquake records for applying to the modeled buildings

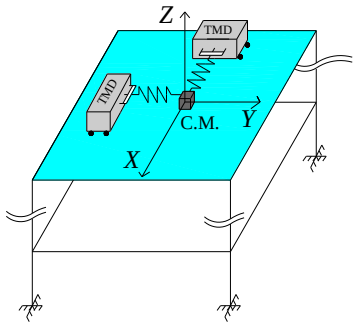

Fig. 6 Locations of the installed ATMDs on top floor of the building

be constant throughout the excitation.

5. Numerical studies

In order to investigate the effectiveness of SACM two building models, a five-story building and a fifteen-story building, are considered. Both of the studied buildings are scaled models. Table 1 illustrates properties of the modeled buildings. The damping ratio of the modeled buildings is assumed to be 0.5% in the first three natural vibration modes.

Table 2 Considered cases for applying earthquake excitation

Case	Earthquake record	Earthquake arrival angle with respect to X direction (β)
case 1	El Centro	30
case 2	El Centro	45
case 3	El Centro	60
case 4	El Centro	90
case 5	Kobe	30
case 6	Kobe	45
case 7	Kobe	60
case 8	Kobe	90
case 9	Chi-Chi	30
case 10	Chi-Chi	45
case 11	Chi-Chi	60
case 12	Chi-Chi	90

According to Fig. 5, three of the earthquake records that are commonly used in structural control (Ozbulut *et al.* 2011) are considered for being applied to the modeled buildings (1940 El Centro, 1995 Kobe and 1999 Chi-Chi). Also, these earthquake records are scaled to have a maximum acceleration of 0.1 g. For inspecting the SACM effectiveness, different cases are considered. These cases are listed in Table 2.

For example, in case 1, the El Centro earthquake is applied to the modeled buildings, and the earthquake arrival angle is 30^0 with respect to X direction.

ATMDs are used to control the response of the modeled buildings. As shown in Fig. 6, two ATMDs are installed on the top floor of the modeled buildings, and the force of each ATMD is applied to the mass center of the top floor. The control force of the first ATMD is applied in X direction and the control force of the second ATMD is applied in Y direction.

Table 3 illustrates the values of the R, Q, T, $\overline{T}$ and σ for the modeled buildings. The selected plant output for the SACM is

$$y_p = [\dot{U}_X^{top\ \ floor}, \dot{U}_Y^{top\ \ floor}]^T \tag{57}$$

where $\dot{U}_X^{top\ \ floor}$ and $\dot{U}_Y^{top\ \ floor}$ are the velocities of the top floor center of mass in X and Y directions. Vector Y_{max} in SACM is selected to be (Bitaraf and Hurlebaus 2013)

$$Y_{\max} = [0, 0]^T \tag{58}$$

To compare the SACM performance with the LQR algorithm, the following performance indices are defined

$$J_1 = \frac{\max \left| U_x^{top\ \ floor}(t) \right|}{\max \left| U_{X\ unctrl}^{top\ \ floor}(t) \right|} \tag{59}$$

$$J_2 = \frac{\max\left|\theta^{top\ floor}(t)\right|}{\max\left|\theta^{top\ floor}_{unctrl}(t)\right|} \tag{60}$$

$$J_3 = \frac{\max\left|U^{top\ floor}_{Y}(t)\right|}{\max\left|U^{top\ floor}_{Y\ unctrl}(t)\right|} \tag{61}$$

$$J_4 = \frac{\max\left|\ddot{U}^{top\ floor}_{X}(t)\right|}{\max\left|\ddot{U}^{top\ floor}_{X\ unctrl}(t)\right|} \tag{62}$$

$$J_5 = \frac{\max\left|\ddot{\theta}^{top\ floor}(t)\right|}{\max\left|\ddot{\theta}^{top\ floor}_{unctrl}(t)\right|} \tag{63}$$

$$J_6 = \frac{\max\left|\ddot{U}^{top\ floor}_{Y}(t)\right|}{\max\left|\ddot{U}^{top\ floor}_{Y\ unctrl}(t)\right|} \tag{64}$$

$$J_7 = \frac{\max\left|F^{TMD}_{X}(t)\right|}{W_{total}} \tag{65}$$

$$J_8 = \frac{\max\left|F^{TMD}_{Y}(t)\right|}{W_{total}} \tag{66}$$

where $U^{top\ floor}_{X}(t)$ and $U^{top\ floor}_{Y}(t)$ are displacements of the top floor center of mass in X and Y directions. The variable $\theta^{\text{top floor}}(t)$ is total rotation of the top floor about the Z axis. Also $F^{TMD}_{X}(t)$ and $F^{TMD}_{Y}(t)$ are the applied control forces in X and Y directions. The variables $U^{top\ floor}_{X\ unctrl}(t)$ and $U^{top\ floor}_{Y\ unctrl}(t)$ are the top floor displacements of the uncontrolled building in X and Y directions. The variable $\theta^{top\ floor}_{unctrl}(t)$ is the top floor rotation of the uncontrolled building about the Z axis. Also, W_{total} is the total weight of the building.

5.1 Five-story building

In the five-story building, the saturation limit of the actuators is selected to be 2% of the building's total weight. Fig. 7 shows the time histories of the top floor displacement $(U_{X5}, \theta_5, U_{Y5})$ in case 1. Fig. 8 shows the time histories of the applied control forces in X and Y directions. SACM decreases the top floor displacement in both X and Y directions. Also, the top floor torsion about Z direction is significantly decreased. As seen in Fig. 7, the torsional response of the uncontrolled building reaches high values. Moreover, the results of the SACM and LQR algorithm are very close to each other.

According to the Fig. 9, comparison of SACM and LQR algorithm performance indices, the SACM was successful in reducing the peak displacements and accelerations of the

Table 3 The values of the parameters R, Q, T, $\overline{T}$ and σ in the modeled buildings

five-story building					fifteen-story building				
R	Q	T	$\overline{T}$	σ	R	Q	T	$\overline{T}$	σ
$I_{2\times2}$	$0.75I_{30\times30}$	$4\times10^{-3}I_{7\times7}$	$5\times10^{-3}I_{7\times7}$	0.05	$I_{2\times2}$	$1.6I_{90\times90}$	$4\times10^{-5}I_{7\times7}$	$4\times10^{-2}I_{7\times7}$	0.05

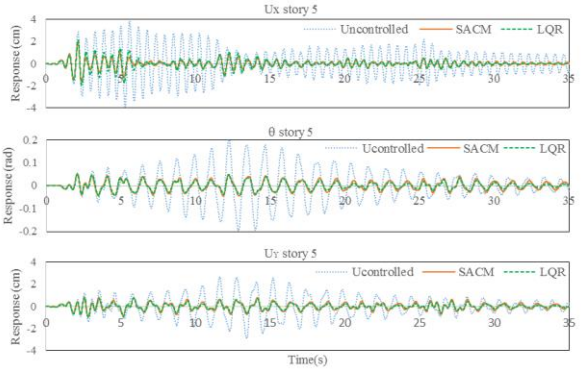

Fig. 7 Time histories of the top floor displacement for the five-story building in case 1

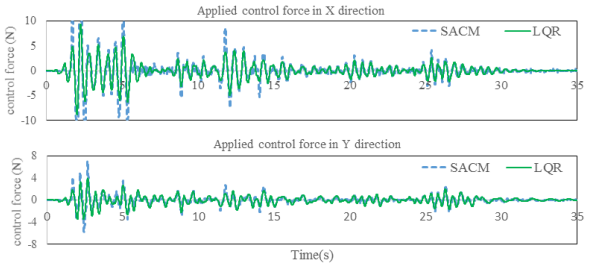

Fig. 8 Time histories of the applied control forces in X and Y directions for five-story building in case 1

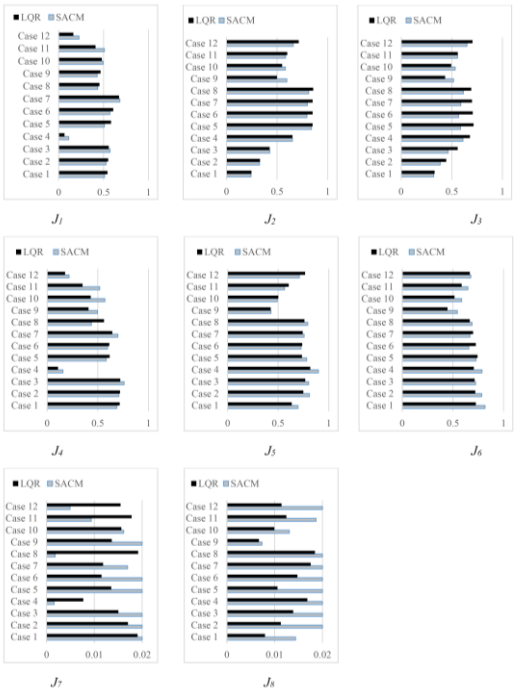

Fig. 9 Performance indices of SACM and LQR algorithm for five-story building

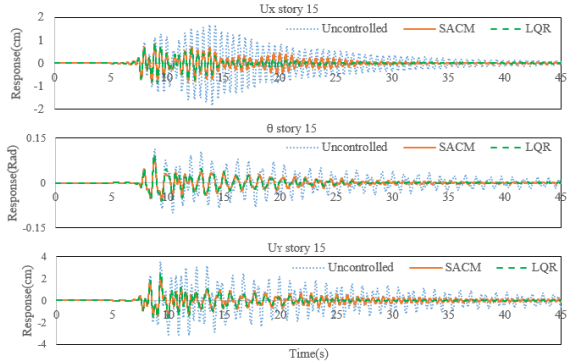

Fig. 10 Time histories of the top floor displacement for the fifteen-story building in case 7

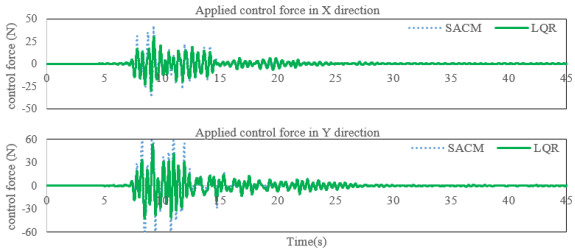

Fig. 11 Time histories of the applied control forces in *X* and *Y* directions for the fifteen-story building in case 7

five-story building in all of the cases. The results of SACM are very close to the results of the LQR algorithm for J_1 to J_6. The results also indicate that SACM reduces the top floor peak displacements in *X* and *Y* directions by 88% to 31%. Moreover, the results show that SACM decreases the top floor peak rotation about the *Z* axis by 76% to 16%. By using SACM, the peak acceleration of the top floor is decreased by 84% to 24% in *X* direction, and the peak acceleration of the top floor is decreased by 45% to 18% in *Y* direction.

5.2 Fifteen-story building

In the fifteen-story building, the selected saturation limit of the actuators was 1.6% of the building's total weight.

Fig. 10 shows the time histories of the top floor displacement $(U_{X15}, \theta_{15}, U_{Y15})$ in case 7. Here again, the results of the SACM and LQR algorithm are seen to be very close. Fig. 11 shows the time histories of the applied control forces in *X* and *Y* directions.

Fig. 12 compares the performance indices of the SACM and LQR algorithm for the fifteen-story building. As shown, the SACM results are very close to the LQR algorithm results for J_1, J_2, J_3, J_5 and J_6. However, the SACM results do differ from LQR algorithm and are far for the J_4 parameter. In case 4, the SACM increases the top floor acceleration in *X* direction (J_4). The parameter J_4 in case 4 of SACM is 1.08. In all other cases, SACM reduces the top floor displacements and accelerations in *X* and *Y* directions. Also, in all of the cases, SACM reduced the top floor rotation about the *Z* axis. Fig. 12 results show that SACM reduces the top floor peak displacements in *X* and *Y*

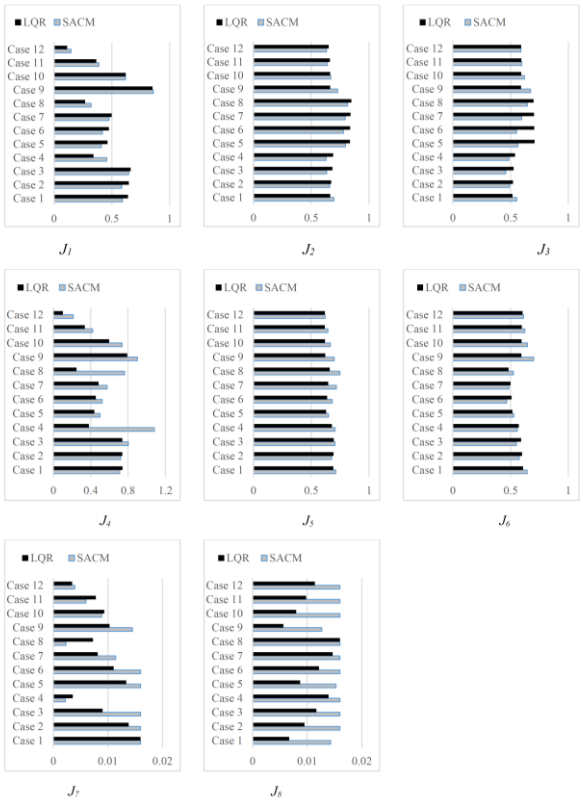

Fig. 12 Performance indices of SACM and LQR algorithm for the fifteen-story building

directions by 85% to 14%. Moreover, the results indicate that SACM decreases the top floor peak rotation about the *Z* axis between 37% and 18%. The SACM decreases the peak acceleration of the top floor by 53% to 30% in *Y* direction.

6. Conclusions

In this study the SACM and LQR algorithm were used to control the response of asymmetric buildings with rotationally non-linear behavior. Unlike the conventional linear approach, the non-linear inertial coupling terms were considered in the motion equations. If rotational non-linearity were considered for the modeled buildings, the buildings would exhibit a different response. The state space equations for the LQR algorithm were updated in each time step, and the control gain matrix was assumed to change through the earthquake excitation. Furthermore, the control gain matrix was updated in each time step. In the modeled buildings, the SACM and LQR algorithm were successful in reducing the top floor displacement and acceleration responses. The SACM and LQR algorithm also reduced the top floor torsional response in the modeled buildings. Unlike LQR algorithm, in SACM it was assumed that the input earthquake excitation is unknown. Moreover, in the SACM, only the velocity vector of the top floor needed to be measured. But in the LQR algorithm, it was assumed that the displacement and velocity of all degrees of freedom were measured in every time step. Also results of the SACM and LQR algorithm were very close to each

other in both of the modeled buildings.

References

Amin Afshar, M. (2009), "Nonlinearities in asymmetric structures", Ph.D. Dissertation, Iran University of Science and Technology, Tehran, Iran.

Amin Afshar, M. and Amini, F. (2012), "Non-linear dynamics of asymmetric structures under 2:2:1 resonance", *J. Non-Lin. Mech.*, **47**(7), 823-835.

Amini, F. and Amin Afshar, M. (2011), "Saturation in asymmetric structures under internal resonance", *Acta Mech.*, **221**, 353-368.

Amini, F. and Javanbakht, M. (2014), "Simple adaptive control of seismically excited structures with MR dampers", *Struct. Eng. Mech.*, **52**(2), 275-290.

Barkana, I. and Guez, A. (1990), "Simple adaptive control for a class of non-linear systems with application to robotics", *J. Contr.*, **52**(1), 77-99.

Barkana, I. and Kaufman, H. (1993), "Simple adaptive control of large flexible space structures", *IEEE Trans. Aerosp. Electr. Syst.*, **29**(4), 1137-1149.

Beer, F.P., Johnston, E.R.J., Eisenberg, E.R. and Cornwell, P.J. (2013), *Vector Mechanics for Engineers: Statics and Dynamics*, 10th Edition, McGraw-Hill, New York, U.S.A.

Bitaraf, M. and Hurlebaus, S. (2013), "Semi-active adaptive control of seismically excited 20-story nonlinear building", *Eng. Struct.*, **56**, 2107-2118.

Bitaraf, M., Hurlebaus, S. and Barroso, L.R. (2012), "Active and semi-active adaptive control for undamaged and damaged building structures under seismic load", *Comput.-Aid. Civil Infrastruct. Eng.*, **27**(1), 48-64.

Bitaraf, M., Ozbulut, O.E., Hurlebaus, S. and Barroso, L. (2010), "Application of semi-active control strategies for seismic protection of buildings with MR dampers", *Eng. Struct.*, **32**(10), 3040-3047.

Gaul, L., Hurlebaus, S., Wirnitzer, J. and Albrecht, H. (2008), "Enhanced damping of lightweight structures by semi-active joints", *Acta Mech.*, **195**, 249-261.

Housner, G.W., Bergman, L.A., Caughey, T.K., Chassiakos, A.G., Claus, R.O., Masri, S.F., Skelton, R.E., Soong, T.T., Spencer, B.F. and Yao, J.T.P. (1997), "Structural control: Past, present, and future", *J. Eng. Mech.*, **123**(9), 897-971.

Khansefid, A. and Ahmadizadeh, M. (2015), "An investigation of the effects of structural nonlinearity on the seismic performance degradation of active and passive control systems used for supplemental energy dissipation", *J. Vibr. Contr.*, **22**(16), 1-11.

Korkmaz, S. (2011), "A review of active structural control: Challenges for engineering informatics", *Comput. Struct.*, **89**(23-24), 2113-2132.

Nazarimofrad, E. and Zahrai, S.M. (2016), "Seismic control of irregular multistory buildings using active tendons considering soil-structure interaction effect", *Soil Dyn. Earthq. Eng.*, **89**, 100-115.

Ozbulut, O.E., Bitaraf, M. and Hurlebaus, S. (2011), "Adaptive control of base-isolated structures against near-field earthquakes using variable friction dampers", *Eng. Struct.*, **33**(12), 3143-3154.

Singh, M.P., Singh, S. and Moreschi, L.M. (2002), "Tuned mass dampers for response control of torsional buildings", *Earthq. Eng. Struct. Dyn.*, **31**(4), 749-769.

Sobel, K., Kaufman, H. and Mabius, L. (1982), "Implicit adaptive control for a class of MIMO systems", *IEEE Trans. Aerosp. Electr. Syst.*, **18**(5), 576-590.

Soong, T.T. and Manolis, G.D. (1987), "Active structures", *J. Struct. Eng.*, **113**(11), 2290-2302.

Yoshida, O. and Dyke, S.J. (2005), "Response control of full-scale irregular buildings using magnetorheological dampers", *J. Struct. Eng.*, **131**(5), 734-742.

Yoshida, O., Dyke, S.J., Giacosa, L.M. and Truman, K.Z. (2003), "Experimental verification of torsional response control of asymmetric buildings using MR dampers", *Earthq. Eng. Struct. Dyn.*, **32**(13), 2085-2105.

CC